

Viewing Angle Compensators for Liquid Crystal Displays based on Layers with a Positive Birefringence

P. VAN DE WITTE*, S. STALLINGA and J. A. M. M. VAN HAAREN
Philips Research Laboratories, Prof. Holstlaan 4, 5656 AA Eindhoven, The Netherlands

(Received April 6, 1999; accepted for publication October 14, 1997)

New compensators to enhance the viewing angle dependence of active matrix twisted nematic displays are designed. In contrast to the well-known discotic compensation films, these compensators are based on layers with a positive birefringence. It is shown that by combining layers with a positive birefringence, the optical properties of layers with a negative birefringence can be mimicked. Expressions are derived that relate the optical properties of the stacks of positively birefringent layers to those of negatively birefringent layers. Calculated conoscopic plots confirmed the correspondence. Two compensator configurations are experimentally tested: the combination of two positively birefringent layers with a tilted optical axis, referred to as $T \times T$ configuration, and the combination of a positively birefringent layer with a planar optical axis and a layer with a tilted optical axis, referred to as the $P \times T$ configuration. In both cases the projections of the optical axes onto the plane of the layers are crossed with respect to each other. It is demonstrated that the compensator based on the $T \times T$ configuration already results in a substantial improvement of the viewing angle of the active matrix display. The contrast values, the linearity of the grey scales, and the color purity of the compensated display for oblique viewing angles are all improved with respect to the non-compensated display. The contrast as a function of viewing angle is further improved by using compensators based on two $P \times T$ layer stacks.

KEYWORDS: liquid crystal display, twisted nematic, compensator, viewing angle

1. Introduction

The narrow viewing cone is one of the main factors limiting the use of active matrix twisted nematic liquid crystal displays (AM-TN LCD) in demanding applications like monitors and televisions. With normally incident light the image quality is very high. At oblique viewing angles the image quality deteriorates. The main problems are the dependence of contrast on viewing angle, loss of grey scale linearity and coloration.

The cause of these problems is the intrinsic angular dependence of the birefringent properties of the liquid crystal layer. This dependence varies as a function of the addressing voltage. Contrast degradation is influenced mostly by the angular dependence of the birefringence of the addressed state. The angular dependence of the optical properties of the liquid crystals at intermediate voltages is the cause of the loss of grey scale linearity. At certain polar angles, states at lower voltages may even show less light transmission than the states at higher voltages. This loss of grey scale linearity is referred to as grey scale inversion. The main causes of coloration are the leakage of light through addressed pixels and the wavelength dependence of the non-addressed state.

Several methods have been proposed for solving the viewing angle problem of TN displays.¹⁻⁴⁾ Solutions that do not influence the complicated manufacturing process of TN displays are preferred. One such solution is to introduce compensation films. The compensation films eliminate the extra birefringence induced by the off-normal viewing angles with respect to the birefringence at normal incidence. Because compensation films are passive components, they can only be used to compensate one liquid crystal state. This fact implies that compensation films cannot fully remedy all viewing angle problems. Because the problems with viewing angle dependence are most severe for the dark states, compensation films are usually designed to compensate the angular dependence of the birefringent properties of the addressed state. A

simple example is shown in Fig. 1.

With displays based on the vertically aligned nematic switching mode, the director of the liquid crystal layer in the non-addressed state is homeotropic. In order to compensate the angular dependence of the liquid crystal layer, the birefringence of the compensator has to be opposite in sign compared to the birefringence of the liquid crystal. This means that the compensator should have an effectively negative birefringence. The required compensator has a low refractive index in the z -direction and high refractive indices in the x - y plane. This type of compensator can be relatively easily obtained through biaxial stretching of polymer films. In the case of TN displays the tilt angle of the molecules in the fully addressed state is much smaller than 90° (Fig. 2). This implicates that the compensator indicated in Fig. 1 is not capable of significantly improving the viewing angle characteristics of

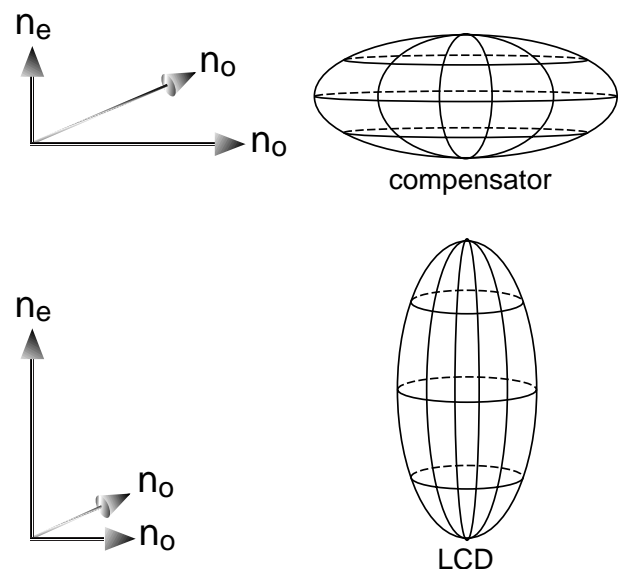


Fig. 1. Compensating principle for vertically aligned nematic displays. The indicatrices for both the compensator and the LCD are shown.

*E-mail address: witte@natlab.research.philips.com

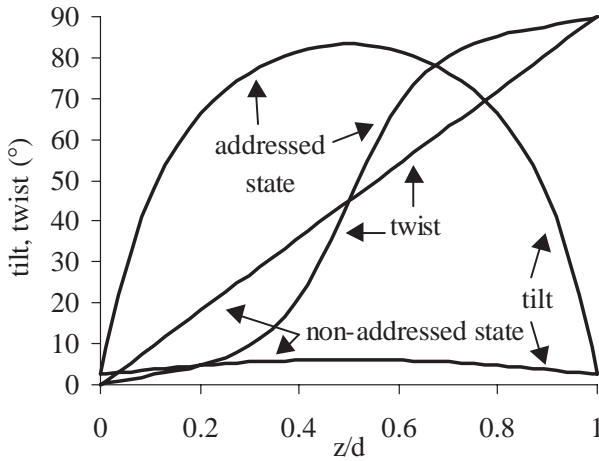


Fig. 2. Twist and tilt of the liquid crystals in an addressed and a non-addressed state of a 90° TN display.

TN displays. For a proper compensation of the angular dependence of the black state, the optical axis of the compensator has to be tilted.

Discotic liquid crystals are a class of materials with intrinsic negative birefringence.^{5,6} Compensation films with a tilted optical axis prepared from discotic liquid crystalline polymers were designed by Fuji Photo Film.^{7,8} The gradient in the orientation of the optical axis of the discotic molecules in the compensator was similar to that of the nematic liquid crystals in the addressed state of the display. These films have been shown to greatly improve the viewing angle dependence of the contrast of TN LCDs.

Compensators with good performance can also be designed on the basis of positively birefringent layers.⁹⁻¹¹ Recently, we demonstrated an effective method for the preparation of layers with a positive birefringence and a tilted optical axis.^{12,13} In this paper we will present results obtained with compensators based on layers with a positive birefringence. We will also describe the theoretical principles for obtaining negatively birefringent layers by stacking positively birefringent layers.

2. Theory

The goal of this section is to consider whether it is possible to approximate the optical properties of negatively birefringent layers with tilted optical axes using positively birefringent layers only. Expressions for the tilt angle and retardation of the positively birefringent layers will be derived in this section on the basis of theoretical considerations. Two different configurations will be analyzed.

- (1) A single negatively birefringent layer with a tilted optical axis has a birefringence that is opposite to that of nematic liquid crystals with a tilted optical axis. This layer will be referred to as D-layer.
- (2) As becomes clear from Fig. 2 the addressed state of the LCD can be approximated by a stack of two positively birefringent layers with the same tilt angles and retarda-

tions and with projections of their optical axes on the plane of the layers that are crossed. Then two negatively birefringent layers with the same tilt angles and retardations and with projections of their optical axes on the plane of the layers that are crossed will have optical properties opposite to those of the LCD. This will be referred to as the D × D configuration.

The theory is based on the generalized 2 × 2 Jones-matrix method in the small birefringence approximation.¹⁴⁻¹⁶ This method is based on neglectation of the effects of reflections and gives quantitatively valid results, provided that the difference between the refractive indices of the neighboring layers and the birefringences of the individual layers are small. In practice this is often the case. According to the method, a stack of *N* birefringent layers is represented by the 2 × 2 Jones-matrix *J* that relates the complex amplitudes of the outgoing *p*- and *s*-polarized waves to the complex amplitudes of the incoming *p*- and *s*-polarized waves:

$$\begin{bmatrix} A_p \\ A_s \end{bmatrix}_{out} = J \begin{bmatrix} A_p \\ A_s \end{bmatrix}_{in} \tag{1}$$

where the Jones-matrix *J* is the product of the *N* Jones-matrices of the individual layers:

$$J = J_N \dots J_2 J_1. \tag{2}$$

Each individual layer acts as a simple retarder. There are two eigenwaves (waves that pass the layer without their polarization being changed); the extraordinary wave with linear polarization *e* and the ordinary wave with linear polarization *o*. The polarization *e* is found by projecting the optical axis *n* onto the plane perpendicular to the propagation direction *k*. The polarization *o* is in the same plane but perpendicular to *e*. The angle *γ* between *e* and the polarization of the *p*-wave *p* then follows from

$$\tan \gamma = \frac{\cos \theta \cos \phi}{\cos \alpha \cos \theta \cos \phi - \sin \alpha \sin \theta} \tag{3}$$

with *θ* being the tilt angle, *φ* the angle between the projection of the optical axis on the plane of the layer and the plane of incidence, and *α* the angle of incidence in the layer. The retardation *μ* (phase difference between the *e*-wave and the *o*-wave) is the product of the magnitude of the wave vector $2\pi/\lambda$, the length of the light path $d/\cos \alpha$ and the effective birefringence $\Delta n \sin^2 \Psi$:

$$\mu = \frac{2\pi d \Delta n \sin^2 \Psi}{\lambda \cos \alpha}. \tag{4}$$

Here, *λ* is the wavelength, *d* the thickness of the layer, *Δn* the birefringence and *Ψ* the angle between the propagation direction *k* and the optical axis *n* defined by:

$$\cos \Psi = \sin \alpha \cos \theta \cos \phi + \cos \alpha \sin \theta. \tag{5}$$

The different vectors and angles are shown in Fig. 3. The Jones-matrix of the layer *l* can now be expressed as:

$$J_l = \begin{bmatrix} \cos(\mu_l/2) + i \sin(\mu_l/2) \cos(2\gamma_l) & i \sin(\mu_l/2) \sin(2\gamma_l) \\ i \sin(\mu_l/2) \sin(2\gamma_l) & \cos(\mu_l/2) - i \sin(\mu_l/2) \cos(2\gamma_l) \end{bmatrix}. \tag{6}$$

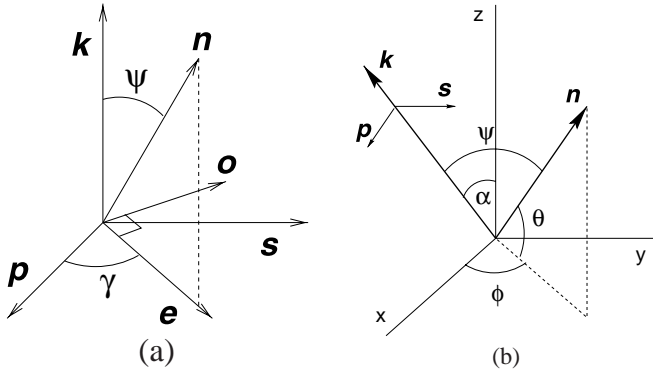


Fig. 3. The relative orientations of the wave vector k , the p and s -polarization vectors p and s , respectively, the e - and o -polarization vectors e and o , respectively, and the optic axis n (left), and the orientation with respect to the space-fixed Cartesian frame (right).

The overall Jones-matrix J can also be expressed in terms of two (orthogonal) eigenwaves and an overall retardation μ (phase difference between the two eigenwaves). The eigenwaves of a stack of different birefringent layers are in general elliptically polarized, not linearly. Formulas (1) to (6) form the basis of the calculation of the polarization change and the transmission as a function of viewing angle and wavelength. Requirements regarding the retardation of the overall Jones-matrix lead to the relation between the negatively birefringent layers and the positively birefringent layers that mimic them. In addition, for normal incidence the retardation layer must cause no polarization change by the retardation layer. In this case the high image quality of the LCD for normal incidence can be maintained. This has two implications: (1) the projection of the optical axis on the plane of a retardation layer must be parallel or perpendicular to the transmitted polarization of the polarizers, and (2) the projections of the negatively birefringent retarders and the positively birefringent retarders that mimic them must be either parallel or perpendicular to each other.

Consider a negatively birefringent layer with a tilted optical axis. The tilt angle is θ_D and the retardation is $(d\Delta n)_D < 0$. When the optical axis is in the plane of incidence, the e -wave and p -wave coincide (like the o -wave and s -wave), since $\phi = 0$. The retardation is:

$$\mu_D = \frac{2\pi(d\Delta n)_D \cos^2(\alpha + \theta_D)}{\lambda \cos \alpha}. \quad (7)$$

The symmetrical properties of the tilted negatively birefringent layer can be approximated by two positively birefringent layers, one with a tilted optical axis, called T-layer, and one with a planar optical axis, called P-layer. The tilt angle and retardation of the T-layer are θ_T and $(d\Delta n)_T > 0$, the retardation of the P-layer is $(d\Delta n)_P$. The requirement regarding the projection of the optical axes on the plane of the layers implies that ϕ must be a multiple of $\pi/2$. We will take $\phi = \pi$ for the T-layer, i.e. the optical axis is in the same azimuthal plane as the optical axis of the D-layer, but tilts in the opposite direction, and $\phi = \pi/2$ for the P-layer, i.e. the optical axis is in the azimuthal plane orthogonal to the plane of the D-layer optical axis. This combination of a P-layer and a T-layer is called a P \times T-configuration. The eigenwaves in the two layers also coincide with the p and s -waves. The overall retardation is therefore:

$$\mu_{P \times T} = \frac{2\pi(d\Delta n)_T \cos^2(\alpha - \theta_T)}{\lambda \cos \alpha} - \frac{2\pi(d\Delta n)_P}{\lambda \cos \alpha}. \quad (8)$$

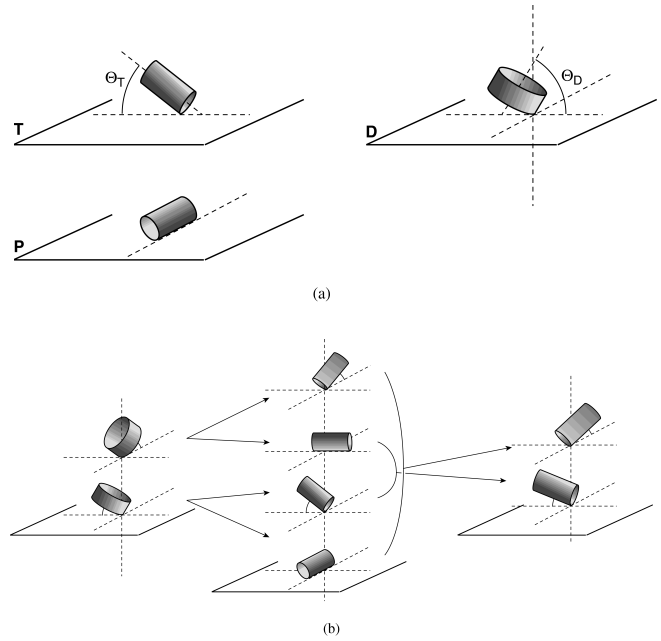


Fig. 4. (a) Schematic representation of the correspondence in the birefringent properties of a D-layer and the P \times T-layers. The extraordinary refractive indices of the P and T-layers point in the same plane as the ordinary refractive index of the D-layer. The ordinary refractive indices of the P \times T layers point in the same direction as the extraordinary refractive index of the D-layer. This shows that the directions of the largest and smallest refractive indices of the P and the T-layers match those of the D-layer. (b) Schematic representation of the design of the compensators. The D \times D layer stack can be approximated by 2 P \times T layers. The two 2 P \times T layers are further approximated by a T \times T layer stack. For further explanations, see text.

From the requirement that the two retardation values are the same ($\mu_D = \mu_{P \times T}$), it follows that:

$$\theta_T = \pi/2 - \theta_D \quad (9)$$

$$(d\Delta n)_P = (d\Delta n)_T = -(d\Delta n)_D. \quad (10)$$

This means that the optical axis of the T-layer is perpendicular to the optical axis of the D-layer, and that the absolute value of the retardations of all layers are the same. The similarity in optical properties is further illustrated in Fig. 4(a).

The quantitative correspondence between the D-layer and the combination of the T-layer and P-layer is exact only if the plane of incidence is the tilting plane of the D and T-layers. If the plane of incidence deviates from this tilting plane, the correspondence is still quite reasonable. This can be seen in Fig. 5, which shows conoscopic plots of the retardations μ_D and $\mu_{P \times T}$.

Now consider the two negatively birefringent layers with crossed projections and the same retardation $d\Delta n < 0$ and tilt angle θ_D (D \times D-configuration). This can be approximated by 2 P \times T combinations [Fig. 4(b)]. For example, if the azimuthal angles of the projections of the optical axes of the D-layers are chosen to be 225° and 315° , then it follows that the corresponding angles for the T-layers as well as for the P-layers must be taken to be 45° and 135° . It proves that a quite reasonable correspondence can be obtained when the P-layer and T-layer at 45° are replaced by a new T-layer, and the P-layer and T-layer at 135° as well. These two new T-layers, with optical axis projections at 45° and 135° , must mimic the D \times D-configuration. The retardation and tilt angle are $(d\Delta n)_T > 0$ and θ_T respectively. The configuration

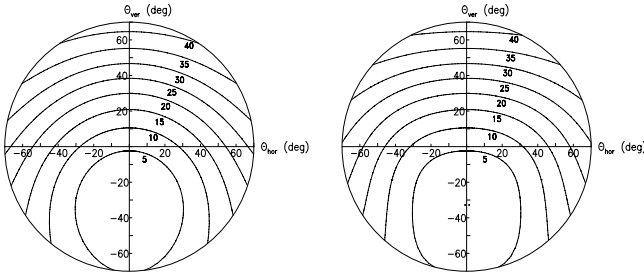


Fig. 5. Conoscopic plots of the retardation (in degrees) of a -150 nm retardation layer with an optic axis at 270° azimuth and 70° tilt (left) and of the combination of two 150 nm retardation layers, one with azimuth 90° and tilt 20° , and one with azimuth 180° and no tilt (right). The wavelength was taken to be 550 nm. The average refractive index of the layers was taken to be 1.5 . The horizontal and vertical viewing angles (θ_{hor} and θ_{ver}) are angles in air.

of the two T-layers can be called a $T \times T$ -configuration. The new T-layer that replaces the $P \times T$ -combination must have approximately the same retardation. Heuristically, the retardation can be set equal to the sum of the retardations of the P-layer and the old T-layer. This implies that the T-layer retardation is twice the absolute value of the individual D-layer retardation:

$$(d\Delta n)_T = -2(d\Delta n)_D. \quad (11)$$

As the T-layer combines the action of the P-layer and the old T-layer, the tilt angle θ_T is larger than zero and smaller than $\pi/2 - \theta_D$. The T-layer tilt is fixed according to the following argument. For the $T \times T$ -configuration it is no longer possible to match the overall retardation $\mu_{T \times T}$ to the overall retardation of the $D \times D$ -configuration $\mu_{D \times D}$ for all directions of incidence in one plane. A match can be made only for some special directions of incidence. It proves that for the $D \times D$ -configuration as well as for the $T \times T$ -configuration there are two directions of incidence at which the overall retardation equals zero. The first direction is a trivial one, namely the direction normal to the layers. The requirement that the second direction be the same for both the $D \times D$ -configuration and the $T \times T$ -configuration defines the T-layer tilt θ_T as a function of the D-layer tilt θ_D . This second direction of incidence can be found in the azimuthal plane bisecting the two projections of the optical axes of the D-layers (or T-layers) on the plane of the layers. In this plane the retardations of the individual D-layers (or T-layers) are the same. The overall retardation is zero when the optical axes appear crossed, i.e. when the e -polarization vectors in the two layers are perpendicular to each other. These vectors are at angles $+\gamma$ and $-\gamma$ with respect to the p -polarization vector, with:

$$\tan \gamma = \frac{\cos \theta_D / \sqrt{2}}{\cos \alpha \cos \theta_D / \sqrt{2} - \sin \alpha \sin \theta_D} \quad (12)$$

because $\phi = \pi/4$ for one D-layer and $\phi = -\pi/4$ for the other. The e -polarization vectors are crossed if $\gamma = \pi/4$ or $\gamma = 3\pi/4$. The second case proves to be the relevant one when the tilt angle is relatively high. This leads to $\tan \gamma = -1$, from which it can be derived that:

$$\alpha = 2 \arctan \left[\frac{1}{\sqrt{2}} \cot \theta_D \right]. \quad (13)$$

A physical solution $\alpha < \pi/2$ is obtained for tilt angles $\theta_D > \arctan(1/\sqrt{2}) = 35.3^\circ$. For the two T-layers $\phi = \pm 3\pi/4$,

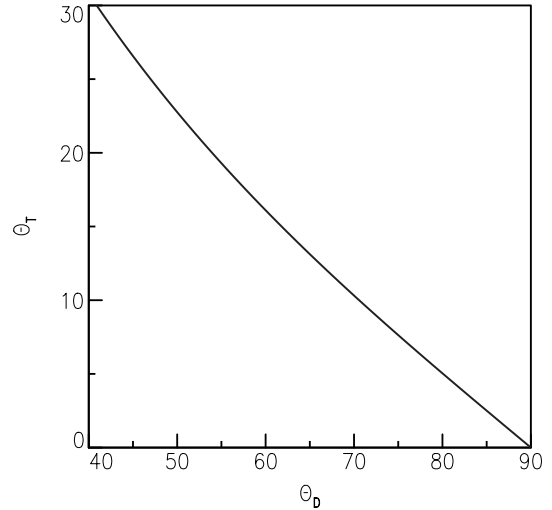


Fig. 6. Tilt angles of the T-layers in the $T \times T$ configuration as a function of the tilt angles of the D-layers in the $D \times D$ configuration.

which, using eq. (3) yields:

$$\tan \gamma = -\frac{\cos \theta_T / \sqrt{2}}{\cos \alpha \cos \theta_T / \sqrt{2} + \sin \alpha \sin \theta_T}. \quad (14)$$

The relevant solution at relatively low tilt angles is again $\gamma = 3\pi/4$, from which it follows that $\tan \gamma = -1$. This can be solved to:

$$\alpha = 2 \arctan[\sqrt{2} \tan \theta_T]. \quad (15)$$

A physical solution $\alpha < \pi/2$ is obtained for tilt angles $\theta_T < \arctan(1/\sqrt{2}) = 35.3^\circ$. The requirement that the retardation values $\mu_{D \times D}$ and $\mu_{T \times T}$ be zero at the same direction of incidence yields to the following relation between the tilt angles:

$$\theta_T = \arctan[\cot \theta_D / 2]. \quad (16)$$

This relation has been plotted in Fig. 6. Clearly, $\theta_T < \pi/2 - \theta_D$, in agreement with our expectations.

This relation between the tilt angles implies a geometrical relation between the optical axes of the D-layers and those of the T-layers. The plane spanned by the two optical axes of the D-layers proves to be perpendicular to the plane spanned by the two optical axes of the T-layers. Figure 7 shows conoscopic plots of the overall retardations of the $D \times D$ -configuration and the $T \times T$ -configuration that approximates it.

The agreement is quite reasonable in view of the heuristic character of the relations between tilt angles and retardations.

3. Preparation of Positively Birefringent Retarders with a Tilted Optical Axis

Two methods have been developed to prepare the films with a tilted optical axis. The first method involves coating liquid crystals on top of high pretilt alignment layers.¹²⁾ This method yields a birefringent layer with a more or less constant tilt angle of the optical axis throughout the layer thickness of the liquid crystals (If K_1 equals K_3 , the tilt angle is really constant). Birefringent layers with a gradient in the tilt angle of the optical axis throughout the layer thickness can be prepared using mixtures of reactive mesogens.¹³⁾ The mixture consists partly of reactive LC molecules with both polar and

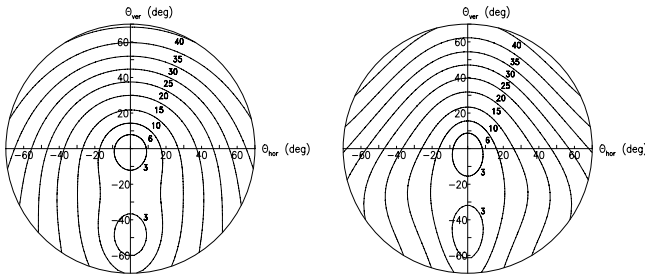


Fig. 7. Conoscopic plots of the overall retardation (in degrees) of a $D \times D$ configuration consisting of D-layers with -100 nm retardation and 70° tilt (left) and of the $T \times T$ configuration consisting of T-layers with 200 nm retardation and 10.3° tilt (right). The azimuth angles of the projections of the D-optical axes are 225° and 270° , whereas the azimuth angles of the T-optical axes are 45° and 135° . The wavelength was taken to be 550 nm. The average refractive index of the layers was taken to be 1.5 . The horizontal and vertical viewing angles (θ_{hor} and θ_{ver}) are angles in air. The polar angle of incidence at which the retardation equals zero is 28.9° in the layers (46.6° in air).

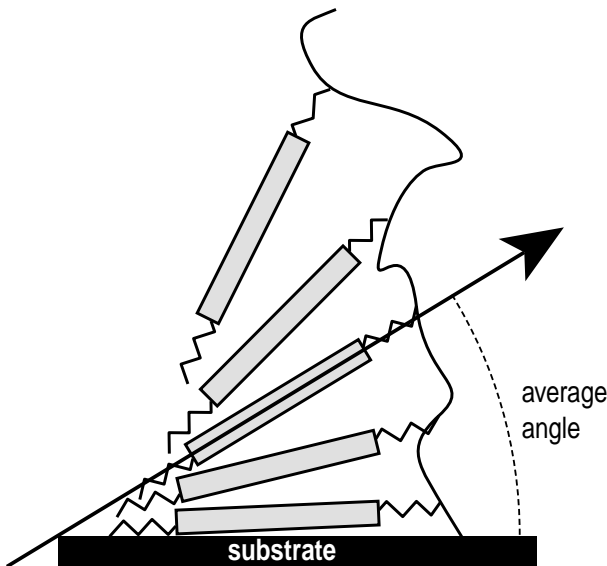


Fig. 8. Schematic representation of a layer based on polymerized nematic liquid crystals. The liquid crystals show a planar to homeotropic transition. This results in a gradient in the optical axis.

apolar groups and partly of an LC crosslinker. The tendency of the polar/apolar molecules to minimize the surface energy causes the molecules to orient homeotropically at air-liquid interfaces. At the substrate an orientation layer is present which causes the molecules to align planarly. In this way a tilt gradient is created (see Fig. 8). In the case studied here, the birefringent layers were prepared on thin glass substrates provided with a polyimide alignment layer.

Because of the presence of gradients in the optical axes of the liquid crystals in the addressed states of the display, only compensators based on layers with a gradient in the optical axis were studied. Layers with different optical properties (like the average tilt angle of the optical axis, retardation) can be obtained by varying the ratio of the compounds or the film thickness (Fig. 9). Details on the influence of various parameters on the retardation profiles can be found in ref. 13.

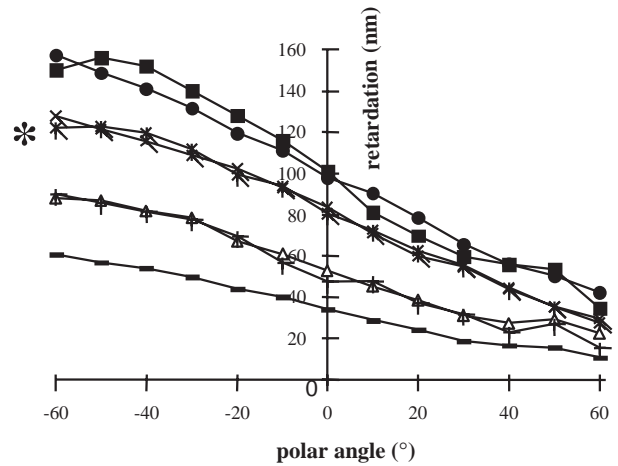


Fig. 9. Retardation profiles of positively birefringent layers with a gradient in the optic axis. The composition of the polymerized liquid crystal layer is kept the same, only the thickness of the layers is varied between 0.2 and $1 \mu\text{m}$.

4. Optical Performance of AM-TN LCDs Provided with Compensators based on Layers with a Positive Birefringence

4.1 Design of compensators

The general principle in the design of compensators is that the optical properties of the compensator are similar but opposite in sign to those of the liquid crystals in the addressed state. As will be clear from Fig. 2 the director profile of the liquid crystals in the addressed state of the LCD is complex. The picture of the director profile of the liquid crystals in the addressed state can be simplified by taking into account that the 90° twist occurs mainly in a small region in the middle of the cell. Therefore, the director pattern of the liquid crystals in the addressed state can be approximated by two layers with a positive birefringence and a tilted optical axis. The projections of the optical axes of the two layers are approximately parallel to the polarizer axes and are crossed with respect to each other. This means that the compensator should consist of two negatively birefringent layers with a tilted optical axis: a $D \times D$ configuration. In §2 it was demonstrated that this configuration can be approximated by two $P \times T$ layer stacks or by one $T \times T$ layer stack. Both configurations have been experimentally tested on active matrix displays.

4.2 Two film configuration: $T \times T$ configuration

There are many ways of positioning two films with a tilt gradient in the display while maintaining the same orientations of the average optical axes. The differences in performance between seemingly similar configurations are still significant but difficult to understand from the basic principles established in the theoretical section. Numerical calculations of the LCD and compensator combination are required to evaluate the differences between these configurations. In the configuration described here, the films are assembled on one side of the display with the planar orientations of the gradient facing each other (Fig. 10). The retardation profiles of the films are indicated with an asterisk in Fig. 9.

The optical properties of the display were measured using DMS equipment (Autronic, Karlsruhe, Germany). The display was an active matrix TFD display obtained from Philips FPD. In Fig. 11(a) the isocontrast plot of the display without

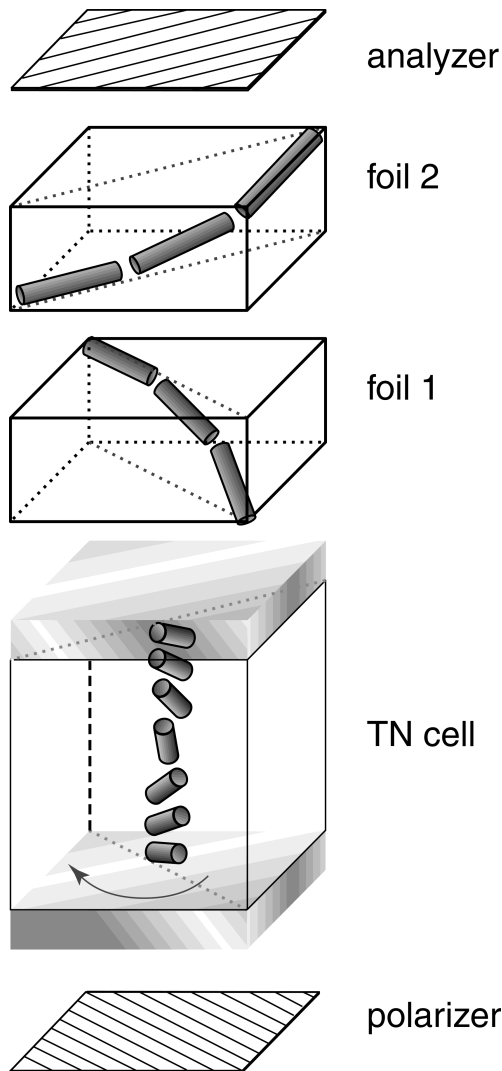


Fig. 10. Positioning of the birefringent layers on the display for the $T \times T$ configuration.

films is shown. The isocontrast area (1 : 10) extends from $+13$ to -33° in the vertical direction. The horizontal viewing angle extends from -55 to $+55^\circ$. Due to the relatively low driving voltages used for driving, the vertical viewing angle is somewhat restricted. On a scale of 8 grey levels the inversion between the 7th and 8th grey level (two darkest grey tones) was measured. This is indicated by the shaded area in Fig. 11. It is clear that a large band of grey scale inversion extends from -11 to -27° in the vertical direction. The features of the film-compensated display are shown in Fig. 11(b). The 1 : 10 isocontrast area now extends vertically from $+35$ to -55° and horizontally from -55 to 55° . The vertical grey scale inversion area has been minimized. The results for the contrasts can be improved further by increasing the driving voltages.

The angular dependencies of the three primary colours and the white state of the film compensated display and the non-compensated display were also measured. Figures 12(a) and 12(b) show the angular dependencies for the horizontal direction.

In the case of the horizontal viewing angles the viewing angle dependence of the colors is minimal in both the film-compensated and the uncompensated display (no yellow coloration). As will be clear from Figs. 12(c) and 12(d), the

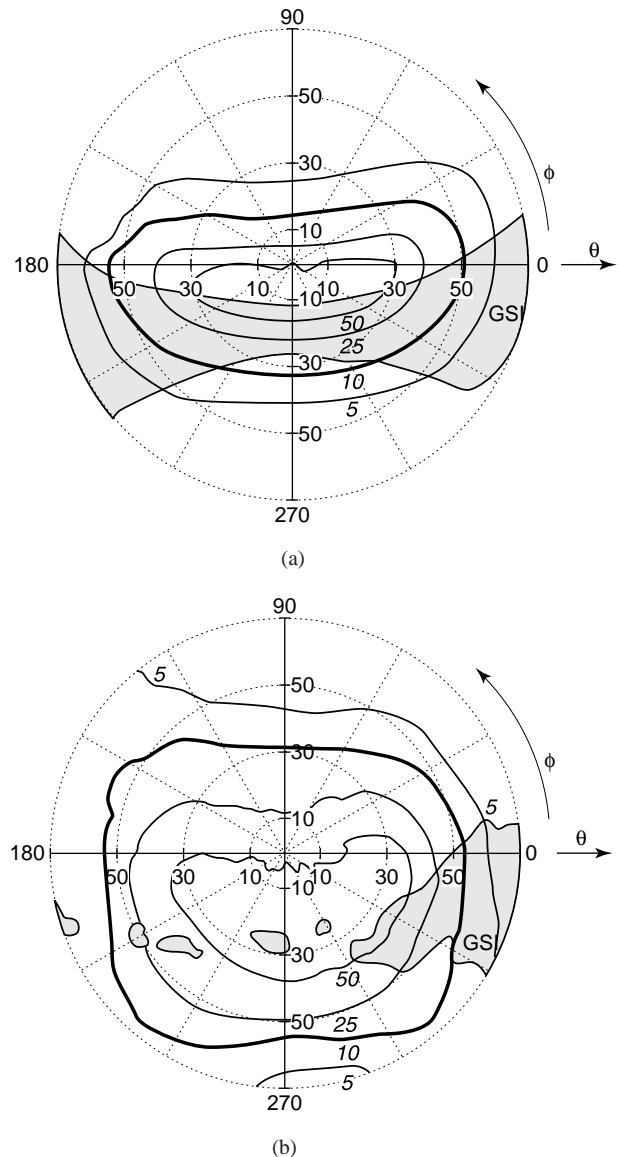


Fig. 11. Isocontrast plots of a display without compensator (a) and a display provided with a $T \times T$ compensator (b). The shaded area indicates the grey scale inversion region.

color saturation of the film-compensated display is considerably better in the vertical direction than the performance of the non-compensated display. This is partly due to the higher values of the contrast. A blue segment is obtained on the screen by fully addressing the red and green pixel. If the leakage of light at high polar angles is less in the case of the red and the green pixels, the purity of the blue color improves. The compensator also reduces the off-normal wavelength dependence of the transmission of the liquid crystal in the non-addressed pixels. This also contributes to the higher purity of the colors. Visual inspection of the displays equipped with these films confirmed the much improved off-normal viewing angle performance of the film-compensated display relative to that of the uncompensated display. It should be noted that Nisseki recently introduced compensators based on architectures similar to those described here.¹⁷⁾

4.3 Four-film configuration: two $P \times T$ combinations

With the four-film configuration the number of ways of positioning the films is even greater. In the case studied here,

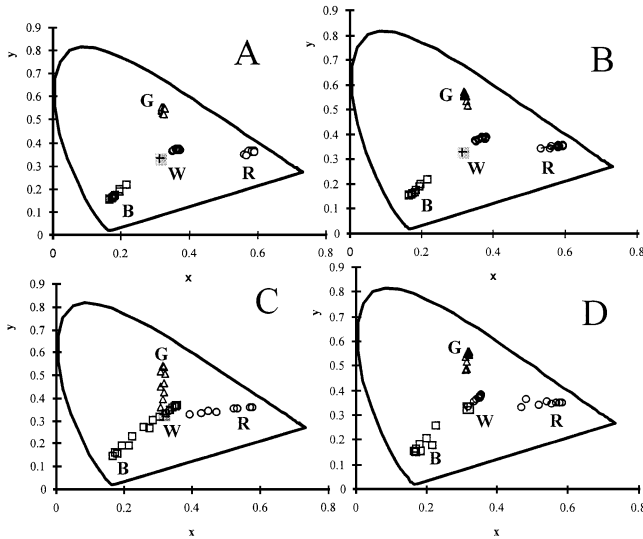


Fig. 12. Color points of the primary colors and the white state obtained for the compensated and the non-compensated display. The data points show both the horizontal and the vertical viewing angles (in 10° increments to ±40° vertical and ±50° horizontal). (a) and (b) represent the viewing angle dependence of the horizontal direction of the uncompensated and the compensated display, respectively. (c) and (d) represent the viewing angle dependence of the vertical direction of the non-compensated and the compensated display, respectively.

the four films were also placed on one side of a TFT display (Fig. 13). Experimental results and numerical calculations showed that other configurations with the same foil parameters gave less favorable results. The retardation of the non-tilted films was 116 nm and the retardation profile obtained for the film with the tilted optical axis is shown in Fig. 13(b). The average tilt of the optical axis of the layer was 29° and the retardation was 110 nm.

The results obtained for the contrast values are shown in Fig. 14. In the horizontal region the contrast values were higher than 10 at polar angles greater than 60°. In the vertical region the contrast values higher than 10 were reached for viewing angles ranging from -45° to over +50°. Especially the horizontal viewing angle is very wide. The grey scale inversion region was further minimized and the color purity of the colors was moreover improved (data not shown here).

5. Discussion and Conclusions

It is clear that the viewing angle performance can be greatly improved by adding compensation films based on positively birefringent layers. Two examples have been given. The simple configuration with two tilted layers is already capable of significantly improving the viewing angle dependence. Even better performance is obtained by adding two non-tilted compensators. We expect that even greater improvements are still possible through detailed optimization of the properties of the films. The performance of the compensators is similar to the performance of compensators based on tilted discotic layers.⁷⁾

An important issue that has not been addressed in this paper is the influence of birefringent substrate layers. In the case studied here the layers were prepared on thin glass substrates. It is also possible to prepare the layers on cellulose triacetate (TAC) substrates. These plastic substrates have an effectively negative birefringence and a homeotropic orientation of the optical axis. Such layers should also be included in the design

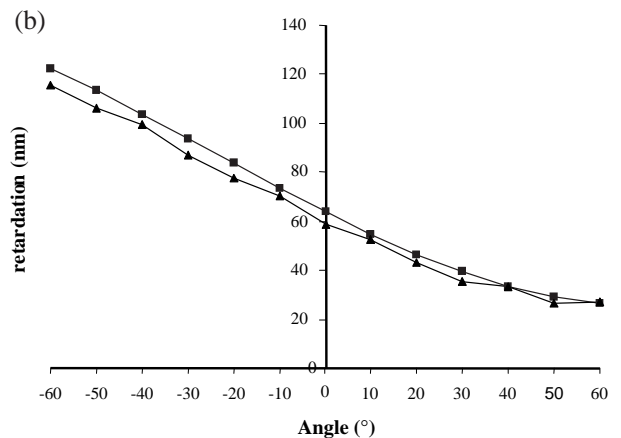
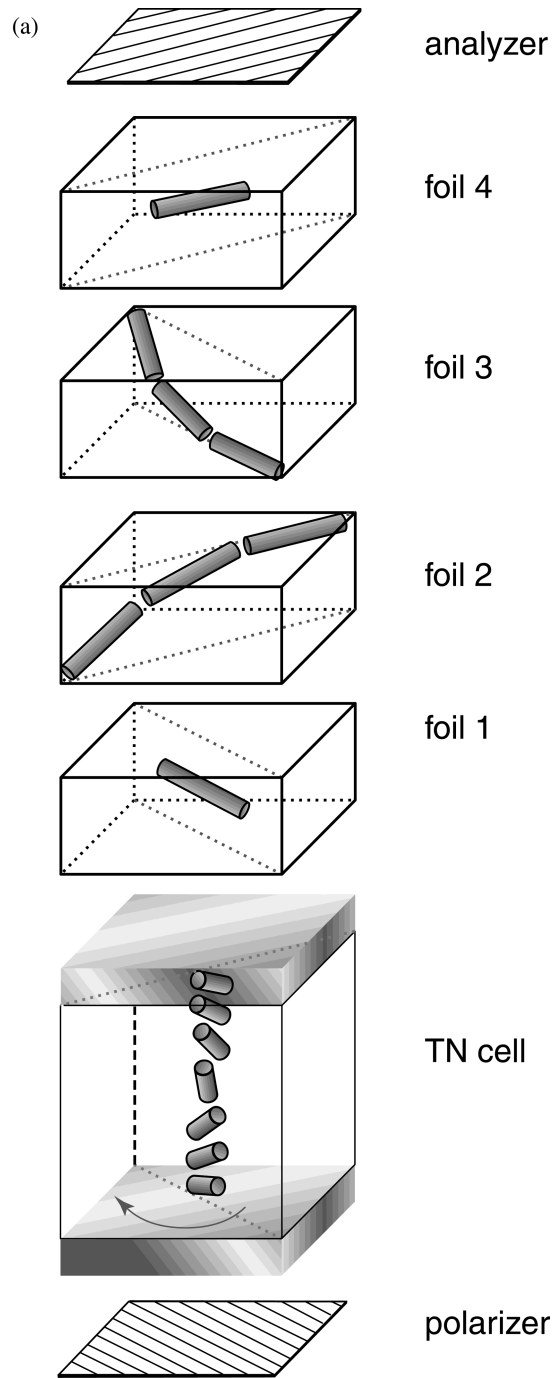


Fig. 13. Foil configuration of the compensator based on 2 P × T combinations. (b) shows the retardation profile of the tilted layer.

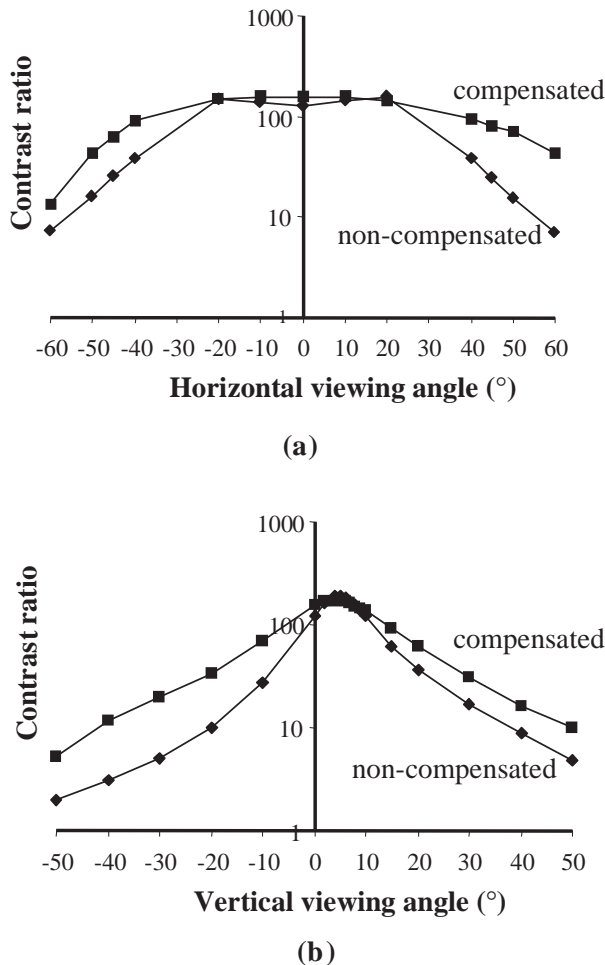


Fig. 14. Contrast ratio as a function of (a) horizontal and (b) vertical viewing angle for the compensator based on $2P \times T$ combinations.

of compensators and can be used to compensate the liquid crystals in the middle of the liquid crystal layer of the display (see Figs. 1 and 2).

The off-normal leakage of light through crossed polarizers is now starting to limit the contrasts. This leakage is due partly to the negatively birefringent TAC substrates used in the polarizers and partly to the fact that the polarizers are no longer crossed at off-normal viewing angles.¹⁸ It has already been shown that this leakage of light can also be reduced by introducing a film with a non-tilted optical axis (a P-layer).¹⁹ Because such films are incorporated in some of the compensator configurations shown here, the optical effect to eliminate the light leakage of polarizers can also be integrated in the design.

These continuous refinements in the design of the compensators give rise to questions regarding the ultimate properties that can be achieved by using compensators. An extensive study has recently been carried out to evaluate to what extent the twisted nematic display can be improved by compensation films.¹⁶ It was shown that almost no limitations exist to improve the horizontal viewing angle dependence. For the vertical viewing angle this does not hold. Two viewing angle problems prove difficult to solve. The first is that brightness and contrast are coupled. Increasing contrasts for the vertical viewing angles will cause the brightness of the white state to decrease at the same viewing angles. The more severe second problem is the fact that the grey scale in-

version problem cannot be completely solved. Especially in the vertical direction, grey scale inversion can be improved by adding compensation films, but it cannot be completely eliminated. This is attributable to the fact that for some directions of view the polarization of light exiting the liquid crystal is identical at two different voltages. The identical polarization states transmitted at these two voltages can be changed by passive birefringent components, but it will be done in the same way for both states. Consequently, the transmission will always be the same at these two voltages. This means that the ideal sequence of grey levels, a monotonous decrease in the transmission with voltage, cannot be achieved for this direction of view. In a case without grey scale inversion, all the grey tones between these two voltages will be approximately equally dark.

Due to the inherent viewing angle dependence of the birefringent properties of liquid crystals, it may be impossible to completely solve the viewing angle dependence of 90° TN displays by compensation films. However, simultaneous optimization of both the liquid crystal switching effect and the compensator may lead to LCDs with an even better viewing angle dependence than can be achieved for TN. Examples were already shown for film-compensated optically compensated bend alignment (OCB) and film-compensated in plane switching (IPS) displays.^{20,21}

Acknowledgements

The authors would like to thank Dick Broer and Frans Leenhouts for helpful discussions and Christianne de Witz for her assistance in the preparation of the layers.

- 1) S. Zimmerman, M. McFraland, J. Wilson, T. J. Credelle, K. Bingaman, P. Ferm and J. T. Yardley: *SID Dig.* (1995) p. 793.
- 2) Y. Koike, T. Kamada, K. Okamoto, M. Ohashi, I. Tomita and M. Okabe: *SID Dig.* (1992) p. 798.
- 3) S. H. Jamal, J. R. Kelly and J. L. West: *Jpn. J. Appl. Phys.* **34** (1995) L1368.
- 4) P. van de Witte, J. C. Galan and J. Lub: *Liq. Cryst.* **24** (1998) 819.
- 5) C. D. Favre-Nicolin and J. Lub: *Macromolecules* **29** (1996) 6143.
- 6) C. D. Favre-Nicolin, J. Lub and P. van der Sluis: *Adv. Mater.* **8** (1996) 1005.
- 7) H. Mori, Y. Itoh, T. Nishiura, T. Nakamura and Y. Shinagawa: *Jpn. J. Appl. Phys.* **36** (1997) 143.
- 8) K. Kawata: *IDW Dig.* (1998) p. 109.
- 9) P. van de Witte, S. Stallinga and J. A. M. M. van Haaren: *SID Dig.* (1997) p. 687.
- 10) P. van de Witte, S. Stallinga and J. A. M. M. van Haaren: *IDW Dig.* (1997) p. 395.
- 11) J. P. Eblen, Jr., L. G. Hale, B. K. Winkler, D. B. Taber, P. Kobrin, W. J. Gunning III, M. C. Skahrolid, T. A. Seder, J. D. Sampic and P. M. Franzen: *SID Dig.* (1997) p. 683.
- 12) P. van de Witte and J. Lub: *Liq. Cryst.* **26** (1999) 1039.
- 13) P. van de Witte, J. van Haaren, J. Tuijtelars, S. Stallinga and J. Lub: *Jpn. J. Appl. Phys.* **38** (1999) 748.
- 14) P. Yeh: *J. Opt. Soc. Am.* **72** (1982) 507.
- 15) C. Gu and P. Yeh: *J. Opt. Soc. Am. A* **10** (1993) 966.
- 16) S. Stallinga, J. M. A. van den Eerenbeemd and J. A. M. M. van Haaren: *Jpn. J. Appl. Phys.* **37** (1998) 560.
- 17) K. Inoue, T. Kurita, E. Yoda, T. Kaminade, T. Toyooka and Y. Kobori: *IDW Dig.* (1998) p. 255.
- 18) H. A. van Sprang: *J. Appl. Phys.* **71** (1992) 4826.
- 19) J. Chen, K.-H. Kim, J.-J. Jyu, J. H. Souk, J. R. Kelly and P. J. Bos: *SID Dig.* (1998) p. 315.
- 20) H. Mori, Y. Itoh, Y. Nishiura, T. Nakamura and Y. Shinagawa: *SID Dig.* (1997) p. 941.
- 21) Y. Saitoh, S. Kimura, K. Kusafuka and H. Shimizu: *Jpn. J. Appl. Phys.* **37** (1998) 4822.